4th International Conference on
Earthquake Geotechnical Engineering
June 25-28, 2007
Paper No. 1594

THE 20 JUNE 1978 THESSALONIKI (NORTHERN GREECE) EARTHQUAKE REVISITED: SLIP DISTRIBUTION AND FORWARD MODELLING OF GEODETIC AND SEISMOLOGICAL OBSERVATIONS

Zafeiria ROUMELIOTI [1], Nikos THEODULIDIS[2], Anastasia KIRATZI[3]

ABSTRACT

We investigate the rupture process of the 20 June 1978 (Mw 6.5) Thessaloniki (northern Greece) earthquake through the application of a linearized least-squares inversion scheme to body-wave phases recorded in the distance range 21º to 37º, and to near-fault levelling data. The inversion of P and S waveforms alone resolved moment release in a single asymmetric patch, confined in an area (~ 16 x 16 km^2), which reaches the surface between the lakes of Langada and Volvi, at the centre of the Mygdonian graben. Peak values of slip are of the order of 2.5 - 3 m and are not observed directly around the hypocenter but are rather shifted ~5 km to WNW above the adopted earthquake focus. The solution obtained from the joint inversion of seismic waveforms and near-source levelling data, additionally to the first patch, resolved moment release in a second patch, confined in a smaller area (~ 9 x 9 km^2) that also reaches the surface beneath Lake Langada. The credibility of the last model is tested in terms of its ability to reproduce geodetic and macroseismic data of the 1978 event. The derived slip distribution pattern is used to compute synthetic static displacements at the surface of the entire meizoseismal area, which are subsequently compared to the existing leveling data and peak ground velocities derived from macroseismic intensity observations. Furthermore, site-specific validation is performed, by forward modeling one strong-motion record of the examined earthquake, recorded at the center of Thessaloniki. Despite the gross character of the computed slip distribution model imposed by the lack of adequate near-fault information, comparisons between predicted and observed data are in an overall satisfactory agreement suggesting the sufficiency of the model for near-source strong ground motion prediction.

Keywords: Thessaloniki earthquake, slip, strong ground motion

INTRODUCTION

In 1978, a sequence of earthquakes occurred in the area of the Mygdonian graben, around 25 km northeast of Thessaloniki, the second largest city in Greece after the capital of Athens (Fig. 1). The intense seismic activity began on 23 May with an earthquake of **M**5.6, continued on 19 June with a **M**5.2 event, and the mainshock occurred on 20 June at night (epicentral parameters 40.739°N - 23.266°E, h=8.0 km; Carver and Bollinger, 1981). The earthquake caused extensive damage to many villages located close to the epicentral area (Stivos, Scholari, Peristeronas, Gerakarou; Fig. 1 for locations), as well as in Thessaloniki, where 38 people died from the collapse of an eight-story

[1] Researcher, Institute of Geodynamics, National Observatory of Athens, Greece, Email: roula@gein.noa.gr
[2] Researcher, Institute of Engineering Seismology & Earthquake Engineering, Thessaloniki, Greece.
[3] Professor, Department of Geophysics, Aristotle University of Thessaloniki, Thessaloniki, Greece.

reinforced concrete building at the centre of the city. In total, the death toll reached the value of 45 people.

The earthquake attracted the attention of many scientists and was extensively studied regarding the aftershock sequence and focal mechanism of the largest events (Kulhánek and Meyer, 1979; Papazachos et al., 1979; Barker and Langston, 1981; Soufleris et al., 1982; more relative references are listed in Table 1), the spatial and temporal distribution of aftershocks (Carver and Bollinger, 1981; Soufleris et al., 1982; Papazachos et al., 1983; Kárnik et al., 1983; Soufleris et al., 1983), the characteristics of strong ground motion (Comninakis et al., 1983; Carydis et al., 1983), the surface ruptures and permanent deformation within the meizoseismal area and the general seismotectonic setting of the earthquakes (Mercier et al., 1979; Andronopoulos et al., 1983; Mercier et al., 1983a,b; Mountrakis et al., 1983; Pavlides and Kilias, 1987; Pavlides et al., 1996; Stiros and Drakos, 2000). Nevertheless, issues related to the details of the rupture process remained unresolved mainly due to constraints posed by the available methods at that time, the sparseness or complete absence of near-source seismological, strong motion and geodetic data and to the poor seismological monitoring of the affected area for a period of at least two weeks after the occurrence of the mainshock.

The aim of this study is to extract information about the rupture process of the 1978 Thessaloniki mainshock by inverting the only available set of seismological data, which consists of waveforms recorded by the High-Gain Long-Period (HGLP) network and the Global Digital Seismograph Network [GDSN; consisting of Seismic Research Observatory (SRO) and Abbreviated Seismic Research Observatory (ASRO) networks at that time]. Although data from regional distances cannot shed light on to the small-scale details of the rupture process, they have been proven capable of revealing the gross characteristic of the slip distribution on faults associated with relatively large earthquakes (e.g. Hartzell et al., 1996; Somerville, 1993; Somerville et al., 1996; Wald et al., 1988). To better resolve our slip distribution model for the 1978 earthquake, we pose some near-fault constraints by incorporating levelling data in our inversions.

THE 1978 THESSALONIKI EARTHQUAKE

The meizoseismal area of the 1978 earthquake practically coincides with a Quaternary basin called the Mygdonia graben (Fig. 1). The basin was formed during lower Miocene within the crystalline mass of the Servomacedonian geological zone and was subsequently filled with Neogene and Quaternary sediments and partly covered with the water of two lakes, namely the Langada and Volvi lakes. The geological history of the graben is associated with NW- and NE-trending strike-slip or oblique normal faults, the most important of which seem to mark the SW margins of the graben, along the coast of the Langada Lake (Mercier et al., 1983a; Pavlides and Kilias, 1987; Tranos et al., 2003).

As inferred from seismological data, the 1978 earthquake sequence was associated mostly with normal faulting (e.g. Papazachos et al., 1979; Carver and Bollinger, 1981; Soufleris et al. 1982). The focal mechanism of the mainshock indicated nearly WNW-trending, NNE-dipping normal faulting (Soufleris and Stewart, 1981) along the SW margin of the graben.

Seismic surface ruptures were observed along three main lines (Fig. 1), the longest of which follows the SW margin of the Mygdonian graben in the area between the two lakes. The other two lines were observed within the sedimentary deposits of the basin and present NW orientation. It has not been proven whether these ruptures were co-seismic or reflected secondary surface effects, although many authors have identified them with the surface expression of the 1978 earthquake fault (e.g. Papazachos et al., 1979; Carver and Bollinger, 1981; Mercier et al., 1983).

Table 1: Source parameters of the 20 June 1978 mainshock previously published. [L = length, W = width, h = focal depth, τ = Rise time, Dur = total duration of the rupture process].

Coordinates φ° N	Coordinates λ° E	Strike/Dip /Rake (°)	L (km)	W (km)	h (km)	u (cm)	M_0(x10^{25}) (dyn·cm)	Δσ (bars)	τ (sec)	Dur. (sec)	Method/ Comment	Reference
		278/46/-70	35	17	6±2	28	5.2±1.8	4		9 ±1.5	Body-wave modelling	Soufleris and Stewart (1981)
						36	5.13	6.6-12		7	Finite difference modelling of the dynamic rupture process	Karakaisis and Mikumo (1993)
			10				3.3		2	6	Iterative deconvolution of teleseismic P waves	Stavrakakis et al. (1987)
		304/80/50									First motions	Papazachos et al. (1979)
			16	17		64	5.2				From empirical relations assuming unilateral rupture	Soufleris et al. (1982)
			28	17		36	5.2				As previous assuming bilateral rupture	Soufleris et al. (1982)
					4-8		5.3			9 ±1.5	Waveform modelling of teleseismic P waves	Soufleris and King (1983)
			32			27	6.6				From spectra	Kulhanek and Meyer (1981)
		286/43/-88			10		2.71					CMT Harvard Catalogue
40.75	23.26											CSEM
40.739	23.229											NEIC
40.784	23.243											ISC
40.710	23.270											AUTH
40.80	23.30											NOA
		288/51/ -	22	14		45	4.2				Forward modelling of geodetic data - model that better fits geodetic and structural data	Stiros and Drakos (2000)
		283/45/ -	17	14		57	4.0				Forward modelling of geodetic data – model that better agrees with seismological estimates	Stiros and Drakos (2000)
40.739	23.266	- /58/ -			8						Aftershock distribution	Carver and Bollinger (1981)
		280/55/-65			11				1	6-8	Moment tensor inversion	Barker and Langston (1981)
40.705	23.266					60	5.25		1.5		Joint inversion of body waveforms and levelling data	This study

CSEM – Centre Sismologique Euro-Méditerrannéen; NEIC – National Earthquake Information Center; ISC- International Seismological Center; AUTH – Aristotle University of Thessaloniki, Dept of Geophysics (on-line catalogue at http://seismology.geo.auth.gr); NOA – National Observatory of Athens (on-line catalogue at http://www.gein.noa.gr)

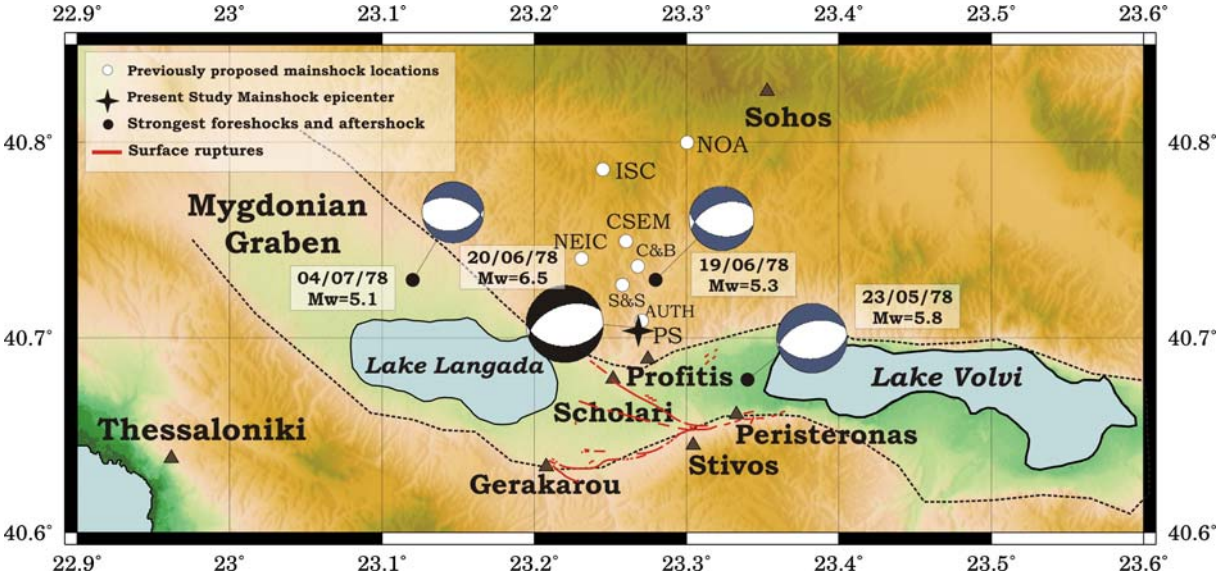

Figure 1. Map showing the broader region of occurrence of the 20 June 1978 (Mw 6.5) earthquake sequence. Open dots denote reported mainshock locations (see Table 1 for agencies; C&B = Carver and Bollinger, 1981; S&S = Soufleris and Stewart, 1981), black star marks our preferred mainshock location obtained in the present study (PS). Focal mechanisms of the mainshock (Liotier, 1989), of two foreshocks (Baker et al., 1997; CMT) and of the largest aftershock of the sequence (Soufleris et al., 1983) are also depicted. The Mygdonian graben (dotted lines) and the three main lines along which surface ruptures were observed (Mountrakis et al., 1983) are also marked in the figure.

FINITE-FAULT SLIP INVERSION

Method

The slip distribution of the 1978 Thessaloniki earthquake is investigated through a linearized least-squares inversion which takes into account the finite dimensions of the source (e.g. Kaverina et al., 2002; Antolik and Dreger, 2003). The fault plane is assigned the orientation of one of the nodal planes implied by the focal mechanism of the examined event and is discretized into a certain number of subfaults. The rupture is assumed to propagate from the hypocenter with constant rupture velocity and each subfault is allowed to rupture only once as the rupture front passes. The slip history of each subfault is represented by an isosceles triangle, while the rake angle is assumed to be constant over the entire fault plane. Synthetic teleseismic waveforms are finally derived as the result of the summation of the individual subfault contributions, using appropriate time delays for both the time needed for the wave to propagate from the hypocenter to the recording stations and the time needed for the rupture front to propagate from the hypocenter to the center of each subfault. The representation of the rupture process is a simplified one that may not be sufficient for a large event that presents spatio-temporal variations of the rupture velocity. However, such a simplified approach is imposed by the nature of the inverted data.

The applied linearized least-squares inversion is combined with slip positivity, spatial gradient smoothing and moment minimization constraints. Taking into account the three constraints, the system of equations to be solved takes the following matrix form:

$$\begin{pmatrix} \mathbf{W}\cdot\mathbf{G} \\ \lambda\mathbf{D} \\ \eta\mathbf{I} \end{pmatrix}(\mathbf{m}) = \begin{pmatrix} \mathbf{W}\cdot\mathbf{d} \\ 0 \\ 0 \end{pmatrix} \quad (1)$$

where **G** is the matrix of the subfault Green's functions, **W** weights the data according to their inverse amplitude and **d** is the data vector. **D** is a gradient smoothing matrix for both the coordinate directions, λ and n are constant smoothing parameters, which are empirically determined, and **m** is the vector of scalar moment values for each subfault. The slip positivity constraint requires that $\mathbf{m} \geq 0$ and thus slip is allowed to occur only along the rake direction, while the moment minimization constraint reduces spurious slip in the later portions of the rupture.

Application of the body-wave waveforms inversion

In the case of the 1978 Thessaloniki earthquake, the initial data set consisted of waveforms from 17 stations of the HGLP and ASRO global networks, which were available by IRIS (Fig. 2). However, we could not use most of these waveforms due to their poor quality and low signal-to-noise ratios at the frequencies of interest. Therefore, the final data vector **d** consists of 5P and 4S waveforms in the distance range 21° to 37°. Initial displacement records were corrected for instrument response and were band-pass filtered between 0.01 and 0.1 Hz. The same filter was also applied to the synthetic Green's functions (**G**), which were calculated using the frequency-wavenumber code of Saikia (1994) and the IASP91 velocity model (Kennett and Engdahl, 1991).

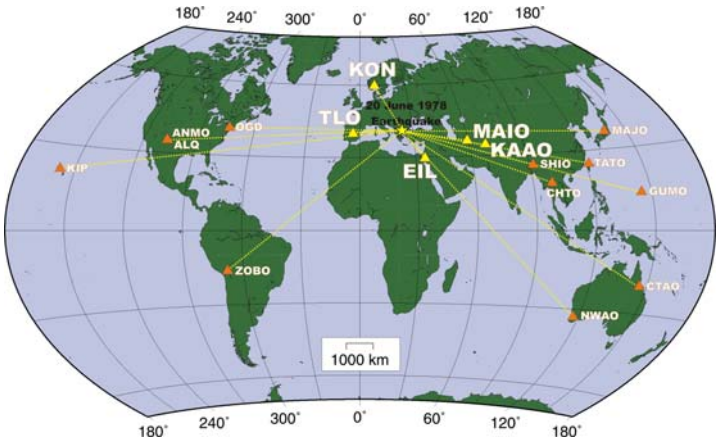

Figure 2. Map showing the locations of the stations that recorded the 1978 Thessaloniki earthquake and their azimuthal distribution with respect to the epicenter of the event. Stations, whose waveforms were finally used in the present study, are KON, TLO, EIL, MAIO and KAAO, marked with larger font size.

The causative fault was represented by a rectangular fault of 35×20 km along strike and dip, respectively. The dimensions of the fault model were chosen based on the distribution of the late aftershocks of the sequence (Carver and Bollinger, 1981; Soufleris et al., 1982) as early aftershocks are not available (local networks were installed in the area about two weeks after the mainshock occurrence, while the permanent network of that time was too sparse to record aftershocks). Distribution of late aftershocks probably defines a larger area that the one that actually ruptured during the mainshock. Therefore, "a priori" we expect to compute a slip distribution that will occupy only a part of the assumed fault area. The fault model area was discretized in 35×20 square subfaults of 1km^2 area.

Table 1 summarizes previously published source parameters of the 1978 mainshock. For our inversions we have adopted the orientation of the north-dipping nodal plane proposed by Soufleris and Stewart (1981), i.e. strike=278º, dip=46º, rake -70º, and for the source depth we used 8 km (Carver and Bollinger, 1981). Regarding the values of rise time, τ, and rupture velocity, V_r, which are fixed during each inversion, we performed a grid search of the parameters model spaces by iterative inversions. Each inversion combined different sets of values for the two parameters within the interval 1.0 – 3.0 sec for the rise time with an increment of 0.5 sec and 2.1 – 3.5 km/sec for the rupture velocity with an increment of 0.2 km/sec. The optimum combination of values, which corresponds to the maximum variance reduction, was found to be τ = 1.5 sec and Vr=2.6 km/sec. The scalar moment

values derived from the inversion were finally converted to equivalent slip values using a rigidity of 3.5×10^{11} dyn/cm^2.

Figure 3a shows our solution derived after multiple inversion tests, which provides satisfactory fit (variance reduction ~ 82%) between the observed and the synthetic waveforms, in most of the examined stations. It consists of one major asymmetric (wider on the upper half) patch, which covers about half of the entire model area (16×16 km^2). Peak values of slip are of the order of 2.5 -3 m and are not observed directly around the hypocenter but are rather shifted 1-2 km to WNW and ~5 km above the adopted earthquake focus.

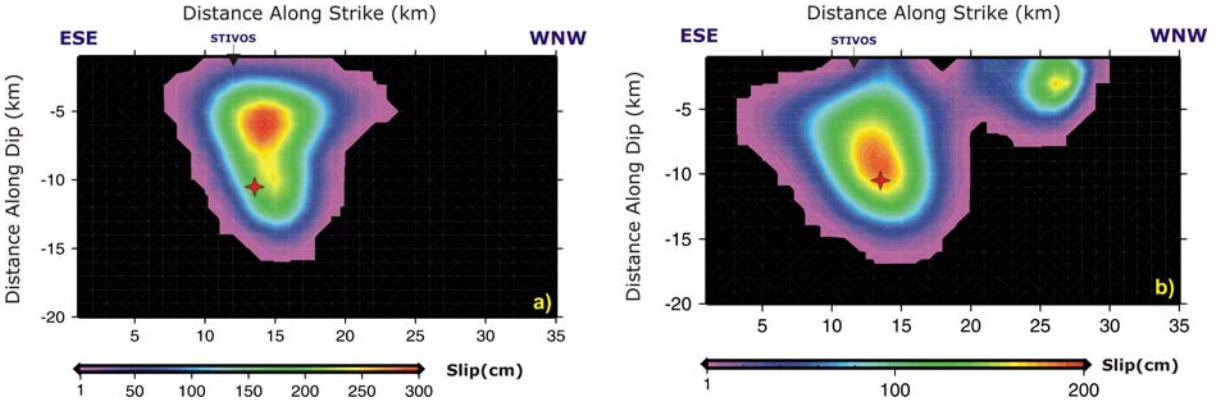

Figure 3. Fault plane view of the slip distribution model of the 1978 Thessaloniki earthquake, as computed from: a) the inversion of P & S waveforms alone and b) the joint inversion of seismic waveforms and geodetic data. In the first case a major slip patch is resolved whereas the joint inversion revealed a second slip patch underneath Lake Langada. Star denotes the mainshock hypocenter. Note that in the first case the strongest moment release (and slip) is not located close to the hypocenter but at shallower depths and 1-2 km to the west.

Application of the joint inversion of body waveforms and levelling data

Stiros and Drakos (2000) examined levelling data from two surveys conducted by the Hellenic Military Geographic Service (HMGS), roughly along the same 110 km long traverse, which crosses the 1978 meizoseismal area, following the southern margin of the Mygdonia graben. One of these surveys was conducted in 1958, well before the 1978 earthquake, and the second one in 1978, few months after the mainshock occurrence. By comparing repeated measurements at 17 benchmarks, common for both surveys, Stiros and Drakos (2000) concluded that the area between the two lakes subsided by up to 25 cm relative to the two ends of the levelling traverse. They also argued that these measurements are significant against random and systematic errors, often appearing in repeated levelling surveys, and attributed the observed subsidence mainly to the tectonic processes associated with the 1978 seismic activity, although they could not rule out a possible contribution from ground instability effects.

The available levelling data can pose the only near-fault constraint for the examined event, even though they may have been contaminated by non co-seismic effects. Luckily, the levelling traverses follow the southern margin of the Mygdonian graben, which most probably coincides with the top edge of the 1978 seismogenic fault. In this sense, these few in number, permanent surface displacements could give additional information for the along-strike distribution of slip during the 1978 earthquake.

The joint inversion of body waveforms and geodetic data involved the same parameterization as in the previous inversions and was also performed by the code of Kaverina et al. (2002), which includes subroutines of Okada (1985). Joint inversions appeared to be much more sensitive to the adopted hypocenter position. The suggested hypocenter locations for the 1978 earthquake, as computed by different seismological centres and researchers (CSEM; ISC; NEIC; AUTH; NOA; Soufleris and Stewart, 1981; Carver and Bollinger, 1981) are depicted in Figure 1. Even in relocated epicentres

(Soufleris and Stewart, 1981; Carver and Bollinger, 1981), the uncertainty in the horizontal direction is of the order of 2-3 km and although such distances are not large enough to affect the results of the regional seismic waveforms inversion, they significantly alter the fit of the near-fault geodetic measurements. Therefore, we tested all the previously published epicentres (Fig. 1 and Table 1) and we additionally performed a grid search in a circle area (of 3 km radius) around them. The northernmost epicentres (those of CSEM, ISC, NOA, Carver and Bollinger, 1981; and NEIC) resulted in poor fit to the observed levelling data (VR<40%) and shifted the top edge of the fault model a couple of kilometres to the north of the observed surface ruptures. On the contrary, the epicentre locations of Soufleris and Stewart (1981) and of Karakostas (1988), the latter being incuded in the on-line catalogue of the Aristotle University of Thessaloniki (AUTH), provided very satisfactory fit (VR>80%) to the geodetic data. Our preferred epicentre location (marked PS in Fig. 1) is 40.705 ^{O}N and 23.266^{O}E, which resulted in a variance reduction of the order of 92% between observed and synthetic levelling data, and almost coincides with the epicentre reported on the AUTH catalogue.

Our preferred epicentre location was used to compute the final slip distribution model through the joint inversion. The model is presented in Figure 3b and provides an overall variance reduction of the order of 87% (83% for the body wave data and 92% for the levelling data). In comparison with the model of Figure 3a, which was based on teleseismic data solely, our final model includes a second smaller slip patch to the west of the main slip concentration. In the first model, the corresponding area includes only a small asymmetry of the computed slip patch, which, nevertheless, does not extend significantly to the west. This second slip patch in the model of Figure 3b is mostly controlled by the high value of subsidence measured at a benchmark located close to the south-western shores of Lake Langada. However, it covers an area of low concentration of earthquake epicentres (see subsequent Figure 5) and increases the along-strike dimension of the ruptured area to values expected by global scaling relations (Wells and Coppersmith, 1994; Papazachos et al., 2004). Due to the fact that slip is distributed in a larger area compared to the previous model, peak slip values are smaller (of the order of 2 m), while average slip throughout the entire ruptured area is ~0.6m. Our final model (Fig. 3b) predicts satisfactory the observed P and S waveforms (Fig. 4b) in most of the examined stations.

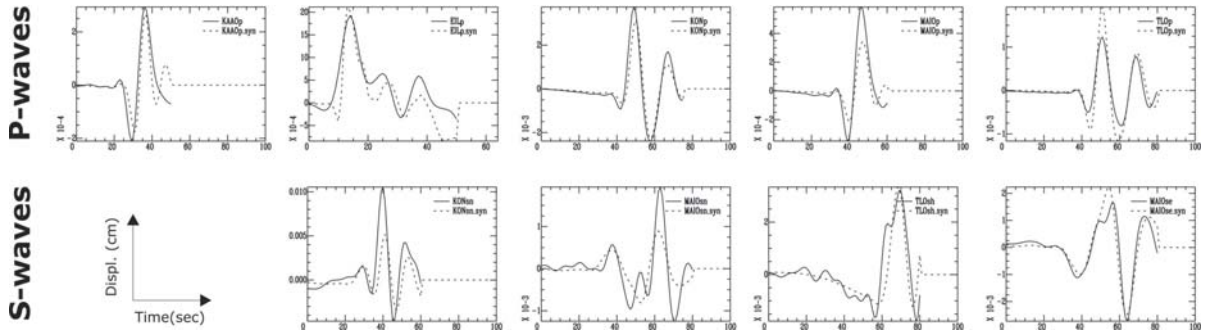

Figure 4. Comparison between observed (continuous lines) and synthetic (dashed lines) P and S waveforms. Synthetics have been calculated using our final slip distribution model (Fig. 3b).

Figure 5 shows the surface projection of our final slip distribution model (Fig. 3b) and superimposed on it are the epicentres of the stronger events of the 1978 sequence. Most of the aftershocks are well outside the areas that ruptured during the mainshock. Such an anti-correlation between aftershocks foci and areas of slip concentration has been observed in many other cases of past earthquakes (Mendoza and Hartzell, 1988).

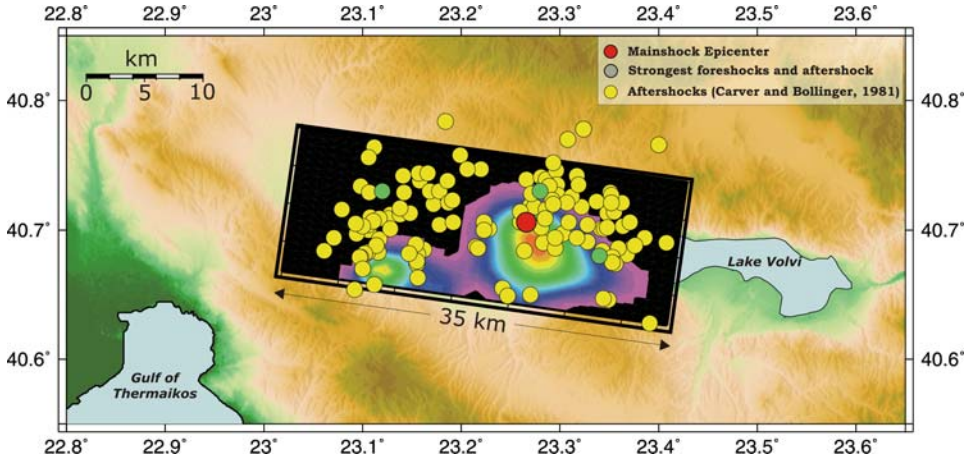

Figure 5. The slip distribution model of Figure 3b is superimposed on the topographic map of the area. Epicenters of foreshocks and aftershocks (yellow and green dots) (Carver and Bollinger, 1981) and of the mainshock (red dot) are also plotted, while white dots show the locations of leveling measurements (Stiros and Drakos, 2000).

VALIDATION TESTS ON THE SLIP DISTRIBUTION MODEL

Synthetic Displacement Field

To test the robustness of the derived slip model (Fig. 3b) we attempted to reproduce the observed amount of subsidence within the meizoseismal area. We used the code of Kaverina et al. (2002) to forward model the static displacement field at the surface. The synthetic static displacement field (Fig. 6a) was compared to the elevation change values suggested by Stiros and Drakos (2000) based on the available geodetic data (Fig. 6b).

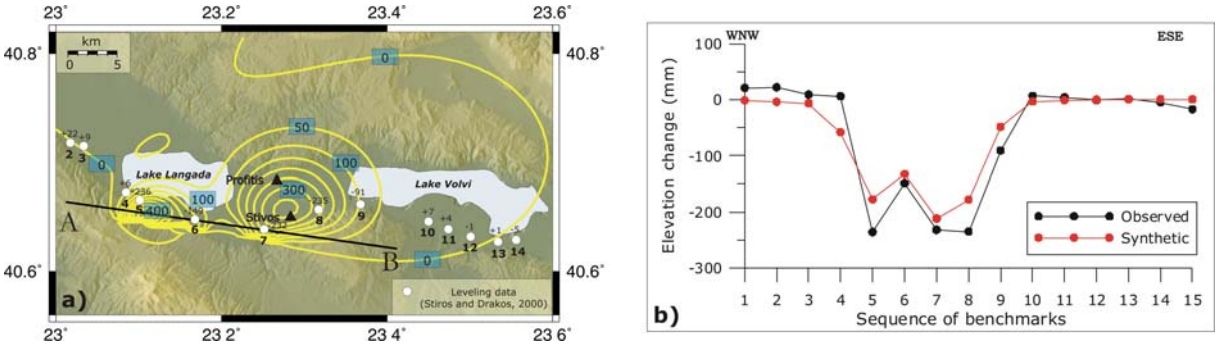

Figure 6. a) Synthetic displacements (in mm) at the surface of the epicentral area using the heterogeneous slip distribution model (Fig. 3b); contours are shown with an increment of 50 mm of elevation change. The locations of the benchmarks of the levelling survey (Stiros and Drakos, 2000) are shown as white dots. Values of elevation changes are shown above each dot. Positive values correspond to uplift of the specific benchmark and negative values to subsidence. Line AB denotes the surface projection of the adopted fault model; b) Cross section to compare observed (black) levelling data (Stiros and Drakos, 2000) with synthetics (red) (also in mm). Positive and negative values of elevation changes as before.

The point-by-point comparison between observed and synthetic values is shown in Fig. 6b. Despite the simplification involved in adopting a simple rectangular fault model and the absence of detailed surface geology from our modelling, we satisfactorily reproduce observed data. Large displacements are predicted within the central-western part of the narrow valley between the Langada and Volvi lakes and underneath the eastern part of lake Langada. These areas of largest surface deformation are

associated with the main slip concentrations of the proposed slip distribution model. During the 1978 earthquake surface ruptures, liquefaction phenomena and extensive damage were also observed in this area.

Observed and predicted strong ground motion parameters

The slip distribution model was also used to simulate strong ground motion parameters within the wider epicentral area. We primarily tried to validate our source model against the available macroseismic intensity data. We computed ground motions using the code of Kaverina et al. (2002) by combining the source model as discussed in previous sections and appropriate theoretical Green's functions. Theoretical Green's function were computed as previously, using the discrete wavenumber code of Saikia (1994), but in this case we used the regional velocity model of Papazachos (1998) applicable to the wider area of study and a cut off frequency of 5 Hz. We performed computations of synthetic velocity time histories at grid points equally spaced (0.04º) to uniformly cover the area depicted in Figure 7a. The peak values contoured in Figure 7a correspond to peak ground velocity (PGV) values obtained by taking the vector sum of the two horizontal components at each grid point. It should be noted that site effects have not been taken into account during these computations.

Simulation results were evaluated using the available observations of macroseismic intensity within the examined area (Papazachos et al., 1997), the distribution of which can be seen in Figure 7a. We used an empirical relation (Theodulidis, 1991) to convert macroseismic intensities (I) to PGV values (Fig, 7b) and to compare them with the PGV values obtained from our modelling.

$$\ln(PGV) = -3.02 + 0.79I - 0.04S$$

where S accounts for site conditions and equals to 1 for "rock" and 0 in cases of "alluvium". The fit between observed and synthetic values is acceptable and large differences observed in some cases, even at sites located at the same distance from the seismic source, can be attributed to factors not accounted for in our modeling (for example site effects, detailed geometry of the seismogenic fault, nonlinear behavior of sediments etc.).

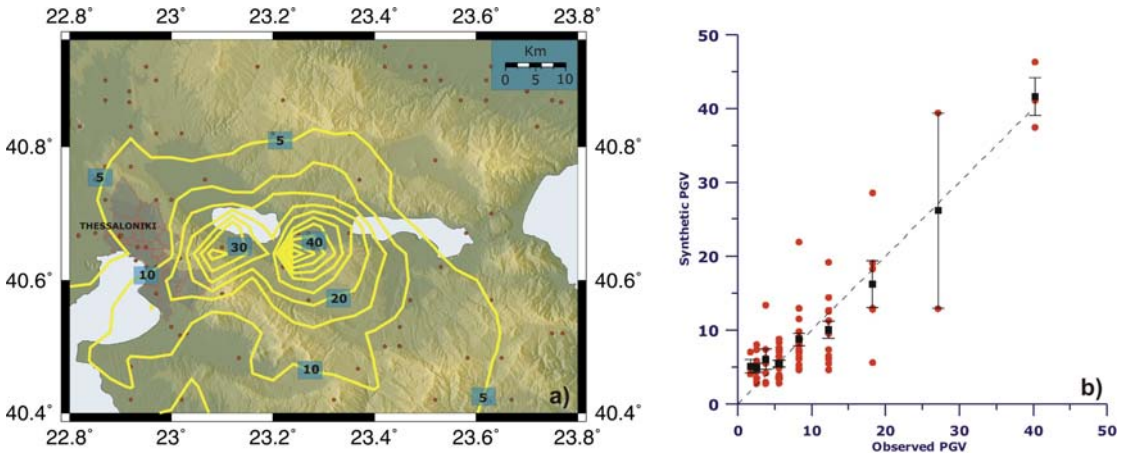

Figure 7. a) Synthetic PGV (in cm/sec) map of the wider epicentral area of the 1978 Thessaloniki earthquake. Contours are presented with an increment of 5 cm/sec. Dots denote the distribution of available macroseismic intensity observations. b) Comparison between synthetic and observed PGV values (in cm/sec), which were computed from macroseismic intensities, using an appropriate empirical relation (Theodulidis, 1991).

In the final stage, we forward calculated the velocity time history for one specific site, which is the site of "City Hotel" within the center of Thessaloniki. At this site, the only strong motion record of the 1978 earthquake was recorded. We limited our forward modelling at relatively low frequencies (<5 Hz) due to limitations posed by the insufficient knowledge of the velocity structure between the source region and the observation point. For this reason, instead of using the original acceleration record, we are using the velocity record obtained by integration of the originally recorded waveform. The

comparison between synthetic and observed records is presented in Figure 8 and their agreement is good in terms of both their peak values and their durations.

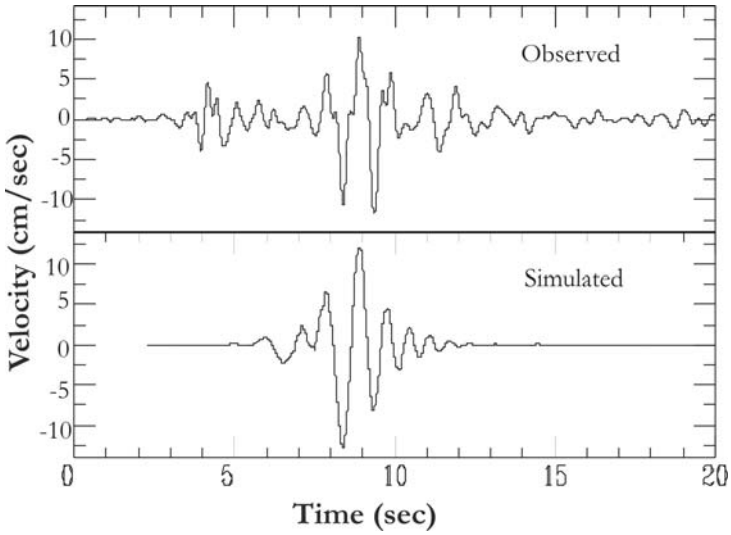

Figure 8. Comparison between observed (top) and synthetic (bottom) velocity record from the 1978 Thessaloniki earthquake at the "City Hotel" site, located at the center of Thessaloniki. The synthetic record is the result of forward modelling using the slip model of Fig. 3b. The match both in amplitude and duration is satisfactory.

CONCLUSIONS AND DISCUSSION

A least-squares inversion of P & S waveform data and leveling measurements was applied to extract information about the rupture process during the 1978 Thessaloniki earthquake. Despite the limited number of clear and thus useable recordings, the satisfactory coverage in azimuth of the 1978 epicenter by the closest stations allowed us to obtain a stable slip distribution model. The inversion of P and S waveforms alone resolved moment release in a single asymmetric patch, confined in an area (~ 16 x 16 km^2), which reaches the surface between the lakes of Langada and Volvi, at the centre of the Mygdonian graben. However, when near-fault constraints were posed by the inversion of available leveling measurements along the southern edge of the seismogenic fault, a second, smaller slip patch was resolved. Thus, the final slip distribution model includes two major concentrations of slip (slip patches). The main slip patch was obtained in the region lying between the lakes of Langada and Volvi and the second one beneath Lake Langada. The area that ruptured is (LxW) 25×15 km^2, peak slip values are of the order of 2 m, while the average slip throughout the ruptured area is estimated to be ~0.6 m. The derived seismic moment from the P & S waveforms inversion is 5.25×10^{25} dyn·cm.

The slip model was validated through its use to forward model static displacements at surface, peak ground velocity distribution within the wider epicentral area, and reproduction of the only acceleration record available.

The synthetic static displacement field successfully predicts the area of maximum elevation change despite the simplicity of the employed fault model. Near-source geodetic data contributed significantly toward the refinement of the along-strike slip distribution pattern. Obviously in the joint inversion the inherent uncertainties of the levelling data propagate into our modelling, as well. These uncertainties refer to several facts, i.e. inverted elevation changes may be contaminated by ground instability effects (Stiros and Drakos, 2000) or reflect the cumulative elevation change by all the large events of the sequence.

Overall, synthetic PGV values were found to agree well with corresponding values empirically derived from macroseismic intensity measurements. The sufficiency of the proposed source model for strong

ground motion simulation was also proven in the case of a site-specific validation at the site of the only available record of the 1978 earthquake within the city of Thessaloniki ("City Hotel"). Although the proposed source model appears to be realistic and capable of reproducing most of the available independent (macroseismic and geodetic) data for the 1978 earthquake, further testing should be pursued. This testing could include, for example, detailed forward modeling of strong ground motion parameters by incorporating specific site effects.

ACKNOWLEDGEMENTS

This work was financially supported by the General Secretariat of Research and Technology (Ministry of Development) of Greece and by the European project "EUROSEISRISK" (EVG1-CT-2001-00040/5-12-2001). Z.R also acknowledges financial support from the State Scholarships Foundation (I.K.Y.) of Greece. We are greatly indebted to D. Dreger from Berkeley University for his continuous cooperation and support, to S. Stiros for providing levelling data and to A. Savvaidis for providing macroseismic intensity measurements. Our colleague Ch. Benetatos is gratefully thanked for his overall help with the inversion code. Most of the figures were produced by the GMT software (Wessel and Smith, 1998).

REFERENCES

Antolik, M. and D. S. Dreger (2003). Rupture process of the 26 January 2001 Mw 7.6 Bhuj, India, earthquake from teleseismic broadband data, Bull. Seism. Soc. Am. **93,** 1235 – 1248.

Andronopoulos, B., A. Eleftheriou and N. Mouyaris (1983). Geological, tectonic and macroseismic study of the area between Thessaloniki and Volvi lake, In: Papazachos, B. C. and P.G. Carydis (eds.), The Thessaloniki, Northern Greece, earthquake of June 20, 1978 and its seismic sequence, Technical Chamber of Greece, 77 – 116.

Baker, C., D. Hatzfeld, H. Lyon-Caen, E. Papadimitriou and A. Rigo (1997). Earthquake mechanisms of the Adriatic Sea and western Greece, Geophys. J. Int. **131,** 559-594.

Barker, J. S. and C. A. Langston (1981). Inversion of teleseismic body waves for the moment tensor of the 1978 Thessaloniki, Greece, earthquake, Bull. Seism. Soc. Am. **71,** 1423 – 1444.

Carydis, P. J. Drakopoulos, S. Pantazopoulou and J. Taflambas (1983). Evaluation of the June 20 and July 5, 1978, Thessaloniki strong motion records, In: Papazachos, B. C. and P.G. Carydis (eds.), The Thessaloniki, Northern Greece, earthquake of June 20, 1978 and its seismic sequence, Technical Chamber of Greece, 231 – 256.

Carver, D. and G. A. Bollinger (1981). Aftershocks of the June 20, 1978, Greece earthquake: a multimode faulting sequence, Tectonophysics **73,** 343 – 363.

CMT, Centroid Moment Tensor Catalog of Harvard, http://www.seismology.harvard.edu/CMTsearch html.

Comninakis, P., Ch. Papaioannou and B. Papazachos (1983). Distribution of macroseismic intensities of the 1978 major earthquakes in Thessaloniki, In: Papazachos, B. C. and P.G. Carydis (eds.), The Thessaloniki, Northern Greece, earthquake of June 20, 1978 and its seismic sequence, Technical Chamber of Greece, 223 – 229.

Dreger, D. and A. Kaverina (2000). Seismic remote sensing for the earthquake source process and near – source strong shaking: a case study of the October 16, 1999 Hector Mine earthquake, Geohys. Res. Lett. **27**, 1941 – 1944.

Hartzell, S. H., and T. H. Heaton (1983). Inversion of strong ground motion and teleseismic waveform data for the fault rupture history of the 1979 Imperial Valley, California, earthquake, Bull. Seism. Soc. Am. **73**, 1553–1583.

Hartzell, S. H., P. Liu and C. Mendoza (1996). The 1994 Northridge California earthquake: Investigation of rupture velocity, rise time, and high-frequency radiation, J. Geophys. Res. **101,** 20,091 – 20,108.

Karakostas, V. (1988). Relation of seismic activity with geological and geo-morphological elements of the wider Aegean area, PhD Thesis, Aristotle University of Thessaloniki, pp. 243.

Kárnik, V., Zd. Schenková and Vl. Schenk (1983). Time variation of the Thessaloniki sequence of 1978, In: Papazachos, B. C. and P.G. Carydis (eds.), The Thessaloniki, Northern Greece, earthquake of June 20, 1978 and its seismic sequence, Technical Chamber of Greece, 151 – 158.

Kaverina, A., D. S. Dreger, and E. Price (2002). The combined inversion of seismic and geodetic data for the source process of the 16 October, 1999 Mw7.1 Hector Mine, California, earthquake, Bull. Seism. Soc. Am. **92,** Special issue on the Hector Mine earthquake, 1266 - 1280.

Kennett, B. L. N. and E. R. Engdahl (1991). Traveltimes for global eartqquake location and phase identification, Geophys. J. Int. **105,** 429–465.

Kikuchi, M. and H. Kanamori (1982). Inversion of complex waves, Bull. Seism. Soc. Am. **72,** 491 – 506.

Kulhánek, O. and K. Meyer (1979). Source parameters of the Volvi – Lagadas earthquake of June 20, 1978, deduced from body-wave spectra at stations Uppsala and Kiruna, Bull. Seism. Soc. Am. **69,** 1289 – 1294.

Liotier, Y. (1989). Modelisation des ondes de volume des seismes se l'arc Ageen, DEA de l'Universite Joseph Fourier, Grenoble, France (in French).

Mendoza, C., and S. H. Hartzell (1988). Aftershock patterns and main shock faulting, Bull. Seism. Soc. Am. **78,** 1438 – 1449.

Mercier, J.-L., N. Mouyaris, C. Simeakis, T. Roundoyannis and C. Angelidis (1979). Intra-plate deformation: a quantitative study of the faults activated by the 1978 Thessaloniki earthquakes, Nature **278,** 45 – 48.

Mercier, J.-L., E. Carey-Gailhardis, N. Mouyaris, K. Simeakis, T. Roundoyanis and C. Anghelidis (1983a). Structural analysis of recent and active faults and regional state of stress in the epicentral area of the 1978 Thessaloniki earthquakes (Northern Greece), Tectonics **2,** 577 – 600.

Mercier, J., E. Carey, C. Simeakis, D. Fondoulis, N. Mouyaris, T. Roundoyannis and Ch. Angelidhis (1983b). Etude des failles neotectoniques et sismiques de la region epicentrale des seismes (Mai – Juin 1978) de Thessalonique (Grèce), In: Papazachos, B. C. and P.G. Carydis (eds.), The Thessaloniki, Northern Greece, earthquake of June 20, 1978 and its seismic sequence, Technical Chamber of Greece, 29 – 76.

Mountrakis, D., A. Psilovikos and B. Papazachos (1983). The geotectonic regime of the 1978 Thessaloniki earthquakes, In: Papazachos, B. C. and P.G. Carydis (eds.), The Thessaloniki, Northern Greece, earthquake of June 20, 1978 and its seismic sequence, Technical Chamber of Greece, 11 – 27.

NOA, National Observatory of Athens, on-line catalogue: http//www.gein.noa.gr

Okada, Y. (1985). Surface deformation to shear and tensile faults in a half space, Bull. Seism. Soc. Am. **75,** 1135 – 1154.

Papazachos, C. B. (1998). Crustal P- and S- velocity structure of the Serbomacedonian Massif (Northern Greece) obtained by non-linear inversion of traveltimes, Geophys. J. Int. **134,** 25 – 39.

Papazachos, B., D. Mountrakis, A. Psilovikos and G. Leventakis (1979). Surface fault traces and fault plane solutions of the May-June 1978 shocks in the Thessaloniki area, North Greece, Tectonophysics **53,** 171 – 183.

Papazachos, B., Th. Tsapanos and D. Panagiotopoulos (1983). The time, magnitude, and space distributions of the 1978 Thessaloniki seismic sequence, In: Papazachos, B. C. and P.G. Carydis (eds.), The Thessaloniki, Northern Greece, earthquake of June 20, 1978 and its seismic sequence, Technical Chamber of Greece, 117 – 131.

Papazachos, B. C., Ch. Papaioannou, C. B. Papazachos and A. S. Savvaidis (1997). Atlas of isoseismal maps for strong shallow earthquakes in Greece and surrounding area (426BC-1995), Ziti Publ., Thessaloniki, pp. 192.

Papazachos, B, E. Scordilis, D. Panagiotopoulos, C. Papazachos and G. Karakaisis (2004). Global relations between seismic fault parameters and earthquakes moment, Proc of the 10th International Congress of Geological Society of Greece, 14 – 17 April, Thessaloniki, Greece.

Pavlides, S. and A. Kilias (1987). Neotectonic and active faults along the Serbomacedonian zone (SE Chalkidiki, Northern Greece), Ann. Tectonicae **1,** 97 – 104.

Pavlides, S., D. Mountrakis, N. Zouros and A. Chatzipetros (1996). Active fault geometry and kinematics in Greece: The Thessaloniki (M_S=6.5, 1978) and Kozani – Grevena (M_S=6.6, 1995) earthquakes – two case studies, Proc. 30th Internat. Geol. Congress, Beijing, China.

Saikia, C. K. (1994). Modified frequency – wavenumber algorithm for regional seismograms using Filon's quadrature: modeling of L_g waves in Eastern North America, Geophys. J. Int. **118,** 142 – 158.

Somerville, P. G. (1993). Engineering applications of strong ground-motion simulation, Tectonophysics **218,** 195 – 219.

Somerville, P., C. K. Saikia, D. Wald and R. Graves (1996). Implications of the Northridge earthquake for strong ground motions from thrust faults, Bull. Seism. Soc. Am. **86,** S115 – S125.

Soufleris, C. and G. Stewart (1981). A source study of the Thessaloniki (northern Greece) 1978 earthquake sequence, Geophys. J. R. astr. Soc **67,** 343 – 358.

Soufleris, C., J. A. Jackson, G. C. P. King, C. P. Spencer and C. H. Scholz (1982). The 1978 earthquake sequence near Thessaloniki (northern Greece), Geophys. J. R. astr. Soc **68,** 429 – 458.

Soufleris, Ch. and G. King (1983). A source study of the largest foreshock (on May 23) and the mainshock (on June 20) of the Thessaloniki 1978 earthquake sequence, In: Papazachos, B. C. and P.G. Carydis (eds.), The Thessaloniki, Northern Greece, earthquake of June 20, 1978 and its seismic sequence, Technical Chamber of Greece, 201 – 222.

Soufleris, Ch., J. Jackson, G. King and C. Spencer (1983). Thessaloniki 1978 earthquakes: locally recorded aftershocks, In: Papazachos, B. C. and P.G. Carydis (eds.), The Thessaloniki, Northern Greece, earthquake of June 20, 1978 and its seismic sequence, Technical Chamber of Greece, 159 – 185.

Stavrakakis, G. N., A.-G. Tselentis and J. Drakopoulos (1987). Iterative deconvolution of teleseismic P waves from the Thessaloniki (N. Greece) earthquake of June 20, 1978, PAGEOPH **124,** 1039 – 1050.

Stiros, S. C. and A. Drakos (2000). Geodetic constraints on the fault pattern of the 1978 Thessaloniki (Northern Greece) earthquake (M_S=6.4), Geophys. J. Int. **143,** 679 – 688.

Theodulidis N. (1991). Contribution to the study of strong ground motion in Greece, PhD thesis, Aristotle University of Thessaloniki, pp. 500.

Tranos, M., Papadimitriou, E. and A.Kilias (2003). Thessaloniki–Gerakarou Fault Zone (TGFZ): the western extension of the 1978 Thessaloniki earthquake fault (Northern Greece) and seismic hazard assessment. Journal of Structural Geology **25**, 2109–2123.

Wald, D. J., and T. H. Heaton (1994). Spatial and temporal distribution of slip for the 1992 Landers, California, earthquake, Bull. Seism. Soc.Am. **84,** 668–691.

Wald, D. J., L. J. Burdick and P. G. Somerville (1988). Simulation of acceleration time histories close to large earthquakes, In: J. Lawrence von Thun (ed.), Earthquake Engineering and Soil Dynamics II: Recent Advances in Ground Motion Evaluation, Geotechnical Special Publication 20, 430 – 444.

Wells, D. L., and K. J. Coppersmith (1994). New empirical relationships among magnitude, rupture length, rupture width, rupture area and surface displacement, Bull. Seism. Soc. Am. **84**, 974-1002.

Wessel, P. and W. H. F. Smith (1998). New improved version of the Generic Mapping Tools released, EOS Trans. AGU 79, 579.